

# Graphene Encapsulated Ni@N/C Catalyst for Highly Selective Semi-hydrogenation of Terminal Alkynes

Jianguo Liu<sup>a, b, d,\*</sup>, Jiangmin Sun<sup>c, d</sup>, Shanshan Lin<sup>d, e</sup>, Longlong Ma<sup>a, d,\*</sup>

<sup>a</sup> Key Laboratory of Energy Thermal Conversion and Control of Ministry of Education, School of Energy and Environment, Southeast University, Nanjing 210096, PR China.

<sup>b</sup> Dalian National Laboratory for Clean Energy, Chinese Academy of Sciences, Dalian 116023, P. R. China.

<sup>c</sup> School of Energy Science and Engineering, University of Science and Technology of China, Hefei 230026, P. R. China.

<sup>d</sup> Guangzhou Institute of Energy Conversion, Chinese Academy of Sciences, Guangzhou 510640, P. R. China.

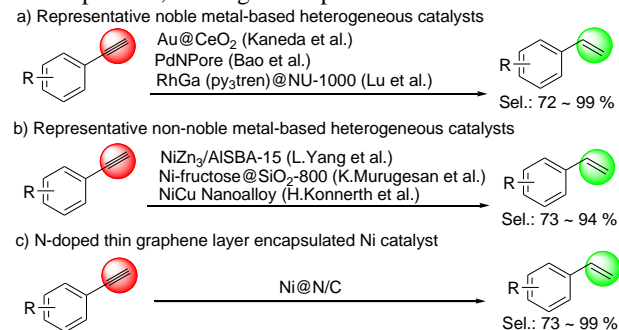
<sup>e</sup> University of Chinese Academy of Sciences, Beijing 100049, P. R. China.

\* Corresponding author: liujg@ms.giec.ac.cn; mall@ms.giec.ac.cn

**KEYWORDS:** Graphene • nitrogen doping • Ni@N/C • semi-hydrogenation • terminal alkynes

**ABSTRACT:** Although precious transition metals such as palladium, platinum, and iridium have been widely used in hydrogenation reactions, the earth-abundant transition metal-catalyzed highly selective semi-hydrogenation of alkynes, especially terminal alkynes to terminal alkenes remains challenging and poor developed. We demonstrate herein that excellent selective, cost-effective semi-hydrogenation of terminal alkynes can be realized via novel none precious graphene encapsulated Ni@N/C catalyst. The precise regulation of the graphene layer for the encapsulated nano-catalyst Ni@N/C can avoid metal leaching and increase catalytic stability significantly. Nitrogen has strong interaction with Ni nanoparticles, which regulate the activity of Ni towards selective semi-hydrogenation of terminal alkynes. The substrate having un-functionalized as well as functionalized substituents, challenging hydrogenation sensitive functional groups (olefins, ketones), were semi-hydrogenated with excellent conversion (up to 99%) and selectivity (up to 99%).

Semi-hydrogenation of alkynes to alkenes represents an important transformation in organic synthesis and has been widely used in the fine chemical industry and petroleum industry.<sup>1-5</sup> It is well known that alkyne could be hydrogenated to alkene easily using transition metal catalyst (Pd, Pt, Rh, Ru, Ir), but normally with undesired over reduction product alkane.<sup>6-9</sup> In the olefin industry, the alkene is the crucial starting material for the synthesis of various valuable products like rubbers and plastics.<sup>10-12</sup> However, during the selective hydrogenation of alkyne to an alkene, starting material alkyne and the over-reduction product alkane are the impurity and harmful components which poisoned the subsequent alkene polymerization process. So, the developments of controllable excellent selective hydrogenation of alkyne to the alkene, which can lower alkyne concentration and increase desired alkene product, are of great importance.<sup>13-16</sup>



**Scheme 1.** Heterogeneous transition metal-catalyzed Semi-hydrogenation of Terminal Alkynes

Up to now, a variety of high efficient transition metal catalysts have been developed and applied in the semi-hydrogenation of alkyne to the alkene, and some of them have been

widely applied in industry. Precious transition metals like Pd, Rh, Ir, Au were widely used in the semi-hydrogenation of internal alkynes, which normally favored Z-selectivity. Recently, many Pd, Au, and Ru catalyzed selective semi-hydrogenation of terminal alkyne, which has been recognized as more challenging substrates than internal alkyne in semi-hydrogenation, have been developed and showed good to excellent catalytic activity and selectivity.<sup>3,14,17-20</sup> Kaneda and co-workers made a great contribution to the Core-Au/Shell-CeO<sub>2</sub> catalyst for the semi-hydrogenation of alkynes.<sup>21</sup> They prepared the novel core-shell nanocomposite Au@CeO<sub>2</sub> catalyst using a facile synthesis redox co-precipitation method through the spontaneous redox reaction between Au(III) with Ce (III) to Au (0) and Ce (IV). The core-shell structure was important for the catalytic activity and stability, it can minimize the exposed surface Au sites and maximize the core-shell interfacial sites. Under mild reaction conditions (Au@CeO<sub>2</sub> (Au: 10 mol%), r.t., 30-50 atm H<sub>2</sub>), various alkynes including aromatic, aliphatic terminal alkynes, and internal alkynes were transformed to alkene product with good to excellent selectivity (72 ~ >99%) (**Scheme 1a**). In 2017, Bao and co-workers<sup>22</sup> reported a heterogeneous palladium(Pd(0)NPore) catalyst for semi-hydrogenation of terminal alkynes. Ten terminal alkynes including aromatic and aliphatic substrates were converted to the desired terminal alkenes in 75~88% yield under mild conditions (1 atm of H<sub>2</sub>, rt). One equiv. NaOH and 16-20 h reaction time were necessary in all the cases (**Scheme 1a**). Recently, Lu et al.<sup>14</sup> reported a novel system containing both active metal Rh (0) and promoter ion Ga (III) on metal-organic framework (MOF) support. The promoter Ga (III) could dramatically affect the

semi-hydrogenation selectivity of the Rh-Ga@NU-1000 catalyst via the electronic (decreasing Rh electron density and making it more electropositive) and structural effect (limiting number of available coordination sites at Rh). Unlike the previous report, the Rh-Ga@NU-1000 catalyst favored high selectivity of E-alkenes from internal alkynes, and also could selective semi-hydrogenated more than 10 examples of terminal alkynes to alkenes with 80 ~ 89 % yield (**Scheme 1a**). Compared with the abovementioned precious transition metal catalysts, earth-abundant transition metal catalysts like Fe, Co, Ni (**Scheme 1b**) also showed promising application in the semi-hydrogenation of alkynes, especially with their obvious advantage in economic cost and bio-safety requirements.<sup>15,16,18,23-29</sup> However, when concerning the most cost-effective and promising heterogeneous supported earth-abundant transition metal catalysts, the unstable and gradually weaken metal-support interaction causing active metal species aggregation during reactions are generally one of the most factors which restrict their wide application in industry. Moreover, the supported metal-based catalysts also suffer from active species leaching in acids or other harsh reaction conditions, results in poor reactivity and selectivity in challenging synthetic organic reactions or poor stability. To solve these problems, recently, the core-shell, yolk-shell structure catalysts that encapsulate active metal nanoparticles (core) with support (shell) maintaining the high activity and stability of metals in the acidic medium are proved to be novel and promising and has recently been applied in a variety of catalytic systems.<sup>30-36</sup> Graphene has been widely used as catalyst support due to its unique properties of thinnest, hardest, thermal and electrical conductivity. But the previous prepared graphene encapsulated catalysts generally have multi-layer of graphitic shell which reduced the catalytic reactivity, hence searching and developing advanced synthesis methods for thin graphene layers especially for twisted bilayer, three-layer graphene with superconductivity are of great interest.<sup>37-40</sup>

Herein, we report a facile and environmentally friendly synthesis of thin graphene shell encapsulated nitrogen doping Ni@N/C catalyst using nickel nitrate and melamine. The catalyst's chemical composition, morphology, phase structure, and its catalytic semi-hydrogenation of terminal alkynes are studied in detail.

The Ni@N/C catalysts were prepared using our previous report with some modification.<sup>41</sup> Briefly, Ni nitrates, citric acid, and different amine sources were mixed in EtOH under vigorous stirring. Then the formed greenish gel was dried and calcined, yielding N-doped graphene encapsulated Ni@N/C catalysts (**Scheme S1**). As shown in **Figure 1** of the representative scanning electron microscopy (SEM) images and transmission electron microscope (TEM) images, different amine sources affected the catalyst's surface significantly. The Ni@N/C-5 catalyst prepared from urea had a denser structure, while the other three catalysts Ni@N/C-1, Ni@N/C-4, Ni@N/C-6 prepared from melamine, ammonium citrate, 1,2 propylene diamine respectively had looser structure, also have the obvious pore structures, this could be further confirmed by the BET measurements of the catalysts. As shown in **Figure 1e-1h**, the nitrogen source can affect the metal nanoparticles' size dramatically. The Ni@N/C-1 has the uniform size of the metal species with 12.5 nm, while the Ni@N/C-4 prepared with ammonium citrate has the smallest particle size 5.9 nm. The Ni@N/C-5 has an uneven metal nanoparticle size, and some of the metal species could be seen aggregation. The Ni@N/C-6 prepared with the aliphatic amine 1,2 propylene diamine has a very irregular metal particle size distribution. The further zoom of the selected area of Ni@N/C catalyst could see the formation of a thin gra-

phene layer structure around the Ni. The catalyst prepared by using melamine has an obvious thin-layer graphene structure, and the graphene wraps the active Ni metal with about 5 numbers of carbon layers. While the catalysts Ni@N/C-4 and Ni@N/C-5 prepared by using ammonium citrate or urea as the nitrogen source have fewer carbon layers, and the structure of the carbon layers is incomplete, and some carbon layers are destroyed. For the catalyst prepared with 1,2 propanediamine, no obvious carbon-coated metal structure was observed, but the presence of a graphene carbon layer was observed. In addition, the TEM-EDS analysis and high-angle annular dark-field EDS (HAADF-EDS) elemental mapping of Ni@N/C-1 exhibited a very similar distribution, which further indicated the co-existence of both N and Ni species in the Ni@N/C-1 catalyst. The elements of C, N, and O were well dispersed over the Ni nanoparticles according to the elemental mapping of the Ni@N/C-1 catalyst, indicating the presence of graphene layers around the nanoparticles. The C, O, N, and Ni atoms were also distributed homogeneously over the other prepared Ni@C catalysts (**Figure S1**).

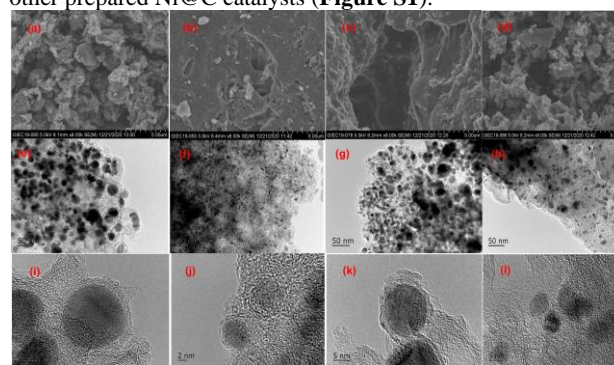


**Figure 1.** Representative SEM images of Ni@N/C-1 (a), Ni@N/C-4 (b), Ni@N/C-5 (c), Ni@N/C-6 (d); Representative HAADF-TEM images of Ni@N/C-1 (e, i), Ni@N/C-4 (f, j), Ni@N/C-5 (g, k), Ni@N/C-6 (h, l).

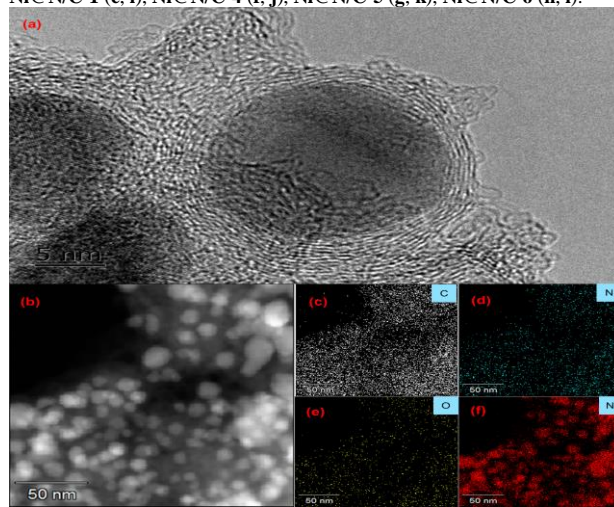


**Figure 2.** Representative HAADF-TEM images of Ni@N/C-1 (a) and corresponding EDS element mapping (EFTEM) of gray, C, N, O, and Ni (b-f).

As shown in the PXRD profile of different catalysts (**Figure 3a**), the Ni@N/C-1 has the highest intensity which showed clearly the Ni (111), Ni (200), Ni (220) metal species. Also, the graphene shell C (002) can be observed, which agrees with the TEM analysis. The intensity of the Ni (111), Ni (200), Ni (220) metal species peaks is lower in the catalysts Ni@N/C-4 and Ni@N/C-6, which indicated that the metal species were dispersed well in the support. While here, it also needs to mention, the nitrogen sources have a great effect on the metal dispersion in the graphene support. The catalyst Ni@N/C-4 which was prepared from ammonium citrate has a higher loading of Ni metal, according to the ICP and SEM-EDS analysis (**Table S1, S2**), but it has better dispersion than

the Ni@N/C-1 catalyst prepared from melamine. For the catalyst Ni@N/C-6, which was prepared from the aliphatic amine 1,2 propylenediamine, it had the lowest Ni loading only 8.36% (Table S2), and also the Ni metal species with smaller nanoparticle size and better dispersion in the support, which following the TEM analysis. The X-ray photoelectron spectroscopy (XPS) was carried out to elucidate the chemical states of the Ni metal elements (Figure 3b-3e). The survey scan of all the catalysts (Ni@N/C-1,4,5,6) showed the presence of Ni, C, O, and N elements. The catalyst Ni@N/C-1 and Ni@N/C-6 had a similar figure trend with the presence of metallic Ni<sup>0</sup> peaks at BE 852.2 eV or 852.3 eV (Ni2p<sub>3/2</sub>) after deconvolution. This was lower binding energy than the reported Ni/AC and the even N doped Ni/AC-N-0.5 catalysts, which indicated that the stronger electron density of the Ni atom in Ni@N/C-1 increased dramatically for the reported two catalysts.<sup>42-44</sup> While the other two Ni@N/C-4 and Ni@N/C-5 had a similar figure trend with the presence of metallic Ni<sup>0</sup> peaks at BE 852.3 eV (Ni2p<sub>3/2</sub>) after deconvolution. Moreover, the presence of a large quantity of high oxidation state of Ni<sup>2+</sup>(II) species was also evident by the peaks at BE 854.3-854.5 eV (Ni2p<sub>3/2</sub>), BE 856.6-857.7 eV (Ni2p<sub>1/2</sub>) and BE 871.3-872.1 eV (Ni2p<sub>3/2</sub>). All of these observations indicated that the active metal species Ni<sup>0</sup> were easily oxidized to Ni<sup>2+</sup>(II) during the preparation. Furthermore, the Ni1s spectrum of Ni@N/C-x was recorded between 395.0 eV and 410.0 eV. Deconvolution of the Ni1s spectra of Ni@N/C-1 can be fitted into three peaks of nitrogen species which were assigned to pyridinic-N, pyrrolic-N, graphitic-N respectively.<sup>28,42,44-46</sup> It is proved that when the N content in the support increased, a charge transfer from N to Ni became more intense. As shown in the TEM-EDS element, when the nitrogen source changed from urea, ammonium citrate, and melamine, the content of N in the catalyst Ni@N/C-5, Ni@N/C-4, Ni@N/C-1 increased from 1.09%, 1.56% to 2.93% gradually. The stronger interaction between the N-doped support and nickel, which comes from the enhanced electron transfer, could improve the stability and activity of the catalyst. As we all know, when the electron acceptor of pyridinic-N species interacts with metal atoms, we can observe the positive binding energy shift. But for when the graphitic-N species donates electrons to the neighboring metal atoms, instead, we can obtain the negative binding energy shift. And this in-censement of electron density could increase the Ni catalyst's selectivity.<sup>43,47</sup> Furthermore, The C1s electrons were deconvoluted into the main four peaks centered at BE 284.2, 285.7, 286.8, 288.3 eV, which can be assigned to graphitic carbon C-C sp<sup>2</sup>, C-C sp<sup>3</sup>/C-N, C-O, and C=O type of carbons respectively.<sup>28,48,49</sup> To know the surface physical properties of the catalysts, we carried out the nitrogen adsorption isotherms of series Ni@N/C catalysts' samples. As illustrated in Figure 3f-3i, all the nitrogen-doped Ni@N/C catalysts showed the typical type IV reversible adsorption isotherm curve, which indicates the existence of mesoporous. The Brunauer-Emmett-Teller surface area of Ni@N/C-1, Ni@N/C-4, Ni@N/C-5, and Ni@N/C-6 was calculated to be 297.6, 435.4, 200.7, and 591.9 m<sup>2</sup>\*g<sup>-1</sup> respectively (Table S3). The nitrogen sources affected the catalysts' BET surface area significantly. The catalyst Ni@N/C-5 prepared from urea has the smallest surface area of 200.1 m<sup>2</sup>\*g<sup>-1</sup>, with the largest pore diameter of 6.03 nm. While for the catalyst Ni@N/C-6 prepared from aliphatic amine 1,2 propylenediamine, it had the largest BET surface area of 591.9 m<sup>2</sup>\*g<sup>-1</sup> and the smallest av-

erage pore diameter of 3.24 nm. Although the Ni@N/C-4 catalyst had a higher loading of Ni (32.1%) than the Ni@N/C-1 catalyst (Ni loading 25.0%), due to its smaller Ni particles and well dispersion in the support, it had a higher BET surface area of 435.4 m<sup>2</sup>\*g<sup>-1</sup> than Ni@N/C-1 catalyst (297.6 m<sup>2</sup>\*g<sup>-1</sup>). According to the quenched solid density functional theory (QSDFT) model, the pore-size distribution of these Ni@N/C-1 samples reveals main peaks in the range of approximately 3 nm to 5 nm. Based on all these characterization results, the following views can be obtained: the most active catalyst, Ni@N/C-1, is characterized by the formation of specific metallic Ni nanoparticles, which are encapsulated in a thin graphene shell.

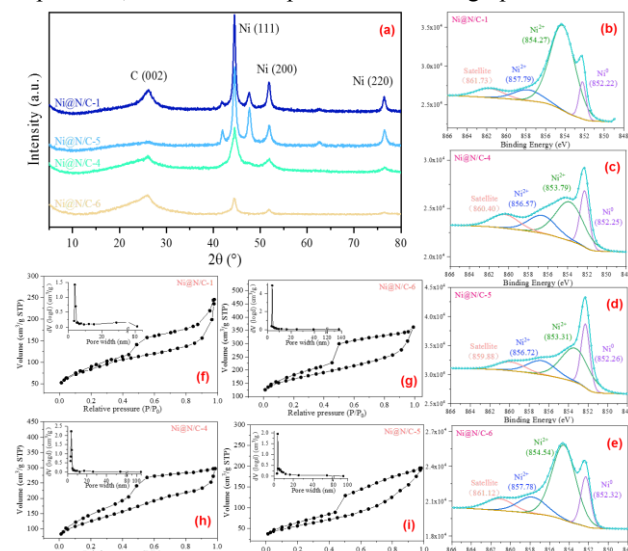


**Figure 3.** Representative XRD images of Ni@N/C-1, Ni@N/C-4, Ni@N/C-5, Ni@N/C-6 (a); representative XPS images of Ni@N/C-1 (b), Ni@N/C-4 (c), Ni@N/C-5 (d), Ni@N/C-6 (e); representative BET measurements of N<sub>2</sub> adsorption and desorption isotherm curves and pore size distribution profile of catalysts Ni@N/C-1 (f), Ni@N/C-4 (h), Ni@N/C-5 (g), Ni@N/C-6 (i). With the successful development of graphene thin layer encapsulated N-doped catalysts (Ni@N/C-x), we were interested in their general application for the semi-hydrogenation of challenging terminal alkynes substrates. Herein, we choose the hydrogenation of phenylacetylene as the standard reaction for the catalysts' activity and reaction conditions' evaluations. As shown in Figure 4a, all the prepared N-doped catalysts were evaluated in the standard reaction conditions. It is clear to see that they gave different catalytic reactivity and product selectivity for the hydrogenation of phenylacetylene. The Ni@N/C-1 gave the best results among the catalysts with 53% of conversion and 94% of **1a** selectivity, and the other over-hydrogenated product selectivity of 6%. The Ni@N/C-4 and Ni@N/C-6 were not active for the semi-hydrogenation of phenylacetylene under the selected reaction conditions. With the optimized catalyst Ni@N/C-1 in hand, we next evaluated the reaction temperature. As illustrated in Figure 4b, the conversion increased from 79% to 99% when the reaction temperature increased from 70 °C to 100 °C, while in the meantime, the **1a** selectivity showed a decreasing trend accordingly. At 80 °C, the Ni@N/C-1 catalyzed semi-hydrogenation of phenylacetylene gave the best results of 92 % conversion and 87 % of **1a** selectivity. Then under this reaction temperature, we shorten and prolonged the reaction time to see the catalytic activity and product distributions. As shown in Figure 4c, when the reaction time was prolonged from 6 h to 9 h, the conversion increased from 86 % to 99%, but the product selectivity decreased from 85 % to 50 %. Although the cyclohexane and CH<sub>3</sub>CN gave excellent selectivity, the catalyst showed low activity in these solvents.

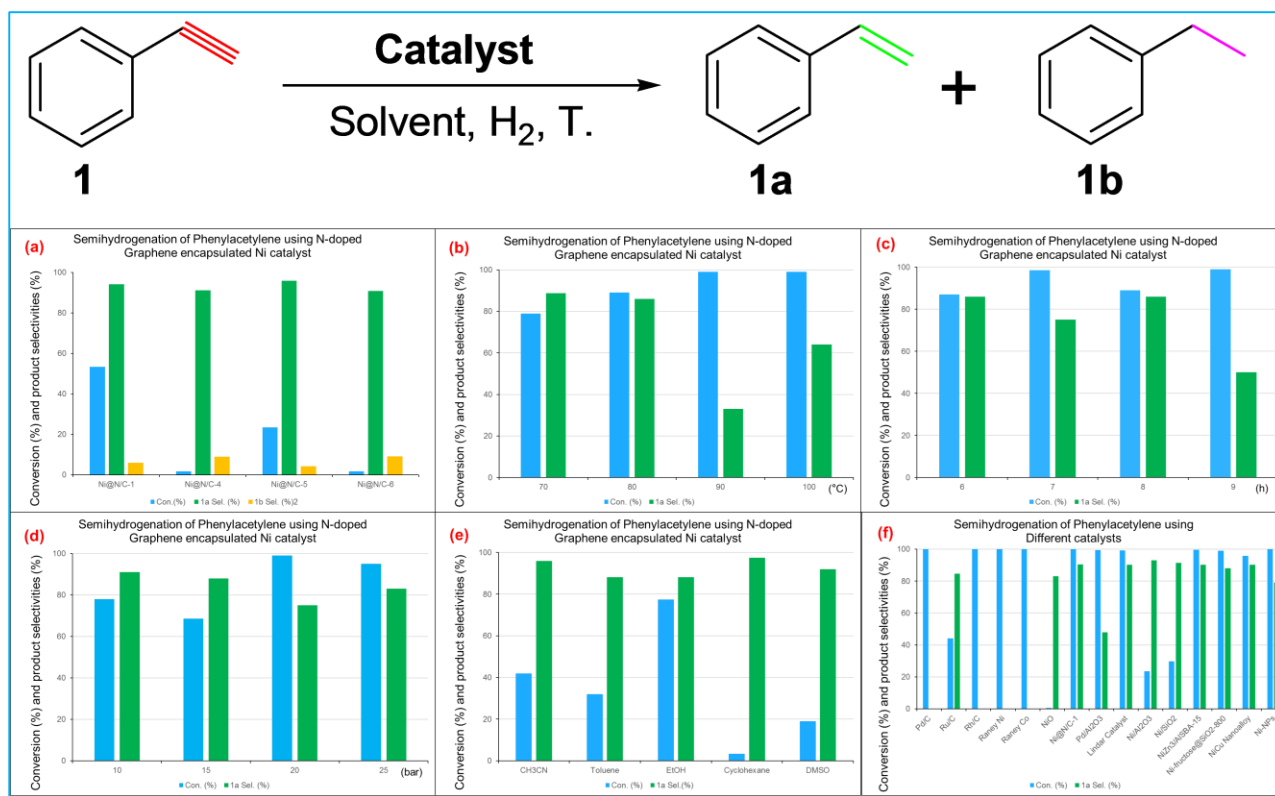


**Figure 4.** Optimization of semi-hydrogenation of Phenylacetylene using N-doped Graphene encapsulated Ni catalyst and comparison with other catalysts. (a) Reaction conditions: 0.5 mmol Phenylacetylene, 5 mg catalyst, 4 ml of MeOH, 20 bar H<sub>2</sub>, r.t. 20 h.; (b) Reaction conditions: 0.5 mmol Phenylacetylene, 5 mg catalyst, 4 ml of MeOH, 20 bar H<sub>2</sub>, 70–100 °C, 8 h.; (c) Reaction conditions: 0.5 mmol Phenylacetylene, 5 mg catalyst, 4 ml of MeOH, 20 bar H<sub>2</sub>, 80 °C, 6–9 h.; (d) Reaction conditions: 0.5 mmol Phenylacetylene, 5 mg catalyst, 4 ml of MeOH, 10–25 bar H<sub>2</sub>, 80 °C, 7 h.; (e) Reaction conditions: 0.5 mmol Phenylacetylene, 5 mg catalyst, 4 ml of solvent, 20 bar H<sub>2</sub>, 80 °C, 7 h.; (f) Reaction conditions: Pd/C, Ru/C, Rh/C, Raney Ni, Raney Co, NiO (0.5 mmol Phenylacetylene, 5 mg catalyst, 4 ml of MeOH, 20 bar H<sub>2</sub>, 80 °C, 7 h); Ni@N/C-1 (10 bar H<sub>2</sub>, 70 °C, 8 h); Pd/Al<sub>2</sub>O<sub>3</sub> (5 wt% phenylacetylene in MeOH, 1 bar H<sub>2</sub>, 40 °C, 1.3 h); Lindlar catalyst (5 wt% phenylacetylene in MeOH, 1 bar H<sub>2</sub>, 40 °C, 30 h); Ni/Al<sub>2</sub>O<sub>3</sub> (5 wt% phenylacetylene in MeOH, 10 wt% Ni loading, 1 bar H<sub>2</sub>, 40 °C, 15 h); Ni/SiO<sub>2</sub> (5 wt% phenylacetylene in MeOH, 10 wt% Ni loading, 1 bar H<sub>2</sub>, 40 °C, 15 h); NiZn<sub>3</sub>/AISBA-15 (40) (5 wt% phenylacetylene in MeOH, 1 bar H<sub>2</sub>, 40 °C, 15.5 h); Ni-fructose@SiO<sub>2</sub>-800 (1 mmol phenylacetylene, 8 mg catalyst (0.6 mol% Ni), 2 ml CH<sub>3</sub>CN, 10 bar H<sub>2</sub>, 110 °C, 5 h); NiCu Nanoalloy (0.005 mol, 50 mg pre-NiCu/MMO, isopropanol, 4 bar H<sub>2</sub>, 100 °C, 3 h); Ni-NPs (0.38 mmol Phenylacetylene, 10.5 mg [Ni(COD)<sub>2</sub>] in 0.15 g ionic liquid [CNC<sub>3</sub>MMM]NTf<sub>2</sub> prepared in situ, 0.5 mL cyclohexane, 4 bar H<sub>2</sub>, 30 °C, 3 h); The conversion and selectivity were determined by GC or NMR analysis using internal standard or reported in the literature.

Furthermore, to showcase the generality and selectivity of this novel N-doped graphene layer encapsulated Ni-based nano-catalyst, its reactivity was compared with other commercially available catalysts, the Lindlar catalyst, and some representative recently reported catalysts<sup>27,50–52</sup>. As illustrated in Figure 4f, the commercially noble catalysts Pd/C, Rh/C, Raney Ni, and Raney Co, which were usually used as hydrogenation catalysts due to their excellent hydrogenation ability, gave the full conversion of the semi-hydrogenation of phenylacetylene but with the over-hydrogenated alkane product. The less active Ru/C catalyst gave 40% conversion and 85% 1a selectivity. The NiO was not active for the phenylacetylene semi-hydrogenation during the selected reaction condition. With a slight modification of reaction conditions (10 bar H<sub>2</sub>, 70 °C, 8 h), the Ni@N/C-1 exhibited excellent reactivity of 99% conversion and comparable excellent selectivity of 91%. The prepared Pd/Al<sub>2</sub>O<sub>3</sub> had excellent activity but with a low selectivity (47.8%) under mild reaction conditions (1 bar H<sub>2</sub>, 40 °C, 1.3 h). Although the commercially widely used catalyst Lindlar catalyst shows a high selectivity (90.2%) and super activity (99% con.), the reaction needs a long reaction time of up to 30 hours. Although the other two Ni-based catalysts Ni/Al<sub>2</sub>O<sub>3</sub> and Ni/SiO<sub>2</sub> showed excellent selectivity (93% and 92%) under 1 bar of H<sub>2</sub> pressure and mild reaction temperature of 40 °C, they had lower activity, with conversions of only 23.5% and 29.8%, respectively, even prolonging the reaction time of up to 15 hours. The reported bi-metal NiZn<sub>3</sub>/AISBA-15(40), and NiCu Nanoalloy catalysts gave

the similar 1a selectivity of 90% with 99% and 96% conversion respectively at the modified reaction conditions separately. The in situ prepared Ni-NPs catalyst could also give super reactivity of 100% conversion and moderate 1a selectivity of 79% with the help of ionic liquid under mild reaction conditions. Under slightly harsh reaction conditions (10 bar H<sub>2</sub>, 110 °C, 5 h), the Ni-fructose@SiO<sub>2</sub>-800 catalyst can semi-hydrogenate phenylacetylene with 99% conversion and 88% 1a selectivity.

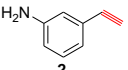
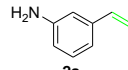
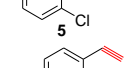
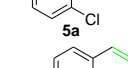
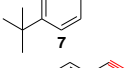
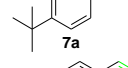
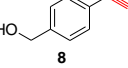
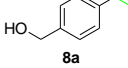
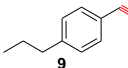
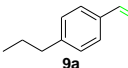
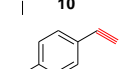
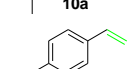
After having the optimized reaction conditions in hand, we then evaluated the substrate scope of Ni@N/C-1 catalyzed semi-hydrogenation reaction. As shown in Table 2, using the Ni@N/C-1 under the optimized reaction conditions of 20 bar H<sub>2</sub>, 80 °C, 7h, most of the aromatic alkynes substrates could be transformed to the corresponding target alkene products with excellent conversion and selectivity (exceeds 99%), which indicating that the graphene encapsulated Ni@N/C-1 catalyst's superior application in the field of non-noble heterogeneous catalyzed semi-hydrogenation reactions. The standard substrate phenylacetylene gave 99% conversion and 75% 1a product selectivity could be obtained under the given standard reaction condition. The 1a selectivity could be increased to 91% under slight modification of the reaction conditions. Then we first investigated the electronic effect of the substituent group on the meta position of aromatic alkynes. For substrate 2 with the electron-withdrawing group -NH<sub>2</sub> on the meta position, full conversion of >99% and 87% selectivity

ity were obtained. The substrate **3** bearing the strongest electron-withdrawing group -F at the *meta* position was a bit difficult to semi-hydrogenate and only gave 61% conversion and 86% **3a** selectivity. While for the other two less electron-withdrawing groups -Br and -Cl, no matter where the substituent group was located on the *meta* or *ortho* position, the catalyst showed excellent catalytic reactivity and product selectivity. We then further examined the effect of changing the substituent group at the *para* position of the aromatic alkynes. Interestingly, substrate **6** with the strongest electron-withdrawing group NO<sub>2</sub> could produce the chemo semi-hydrogenation product **6a** in excellent conversion and good selectivity. The substrate having the strong electron-donating group NMe<sub>2</sub> also gave an excellent conversion of 94% and excellent selectivity of 99%. The substrates with weak electron-donating group t-butyl, N-propyl, only gave moderated conversion but without any over-hydrogenation products. The graphene encapsulated Ni@N/C-1 also showed excellent catalytic reactivity of 93% conversion and 74% selectivity for the *E* isomer product (**12a**). Here it is known that the electron-withdrawing and electron-donating groups can both delocalize the electron negativities of the aromatic ring, which can further affect the terminal alkynes' electron negativity. Here, the substrates have electron-withdrawing groups NH<sub>2</sub>, Br, Cl, NO<sub>2</sub>, NMe<sub>2</sub> gave higher catalytic reactivity and selectivity of the desired semi-hydrogenated product than the substrates with electron-donating groups of t-butyl, N-propyl.

**Table 2. Substrate Scope of Ni@N/C-1 catalyzed semi-hydrogenation of aromatic alkynes**

$$R^1-C\equiv C-R^2 \xrightarrow[\text{MeOH, 80 }^\circ\text{C, 20 bar H}_2, 7 \text{ h}]{\text{Ni@N/C-1}} R^1-CH=CH-R^2 + R^1-CH_2-CH_2-R^2$$

Product a                      Product b

Entry	Substrate	Product	Conv. (%)	Sel. (%)
1			99 99	75 91 <sup>b</sup>
2			99	87
3			61	85
4			98	84
5			99	98
6			99	89
7			43	99
8			91	73
9			63	99
10			94	99
11			99	91
12			93	74

<sup>a</sup> Reaction conditions: 0.5 mmol Phenylacetylene, 5 mg catalyst, 4 ml of MeOH, 20 bar H<sub>2</sub>, r.t. 20 h. <sup>b</sup> Reaction conditions: 0.5 mmol Phenylacetylene, 5 mg catalyst, 4 ml of MeOH, 20 bar H<sub>2</sub>, r.t. 20 h. The conversion and selectivity were determined by GC or NMR analysis using internal standard or reported in the literature.

The Ni@N/C-1 catalyst's stability and recycling test were further carried out in both batch reactor and advanced flow reactor. Surprisingly, the graphene encapsulated Ni@N/C-1 catalyzed semi-hydrogenation of phenylacetylene did not loss significant reactivity and product selectivity after 10 times' recycling test (Table S4). And also it needs to mention, the stable catalyst with magnetic properties can be applied in the industrially applicable flow reactor, and reaction conditions can be optimized easily by switching the control valve. The catalyst showed excellent reactivity and selectivity for the semi-hydrogenation of phenylacetylene in the flow reactor and the catalyst can be recovered easily (Table S5, Scheme S2). The graphene encapsulated Ni-based catalysts semi-hydrogenation in flow reactor process was high environmental friendlier with producing less byproduct and easily recycling use of H<sub>2</sub>. This can provide a feasible reference method for industrialized selective production of ethylene.

## CONCLUSIONS

In summary, we have reported the successful facile synthesis of N-doped thin graphene layer encapsulated Ni-based catalyst. The nitrogen sources had a great effect on the catalyst physical properties and interaction between support and active metal species, which further affected the Ni@N/C catalysts' activity and selectivity for semi-hydrogenation of aromatic alkynes. The optimized Ni@N/C catalyst showed excellent activity and selectivity for semi-hydrogenation of phenylacetylene under mild reaction conditions. More than 10 aromatic alkynes substrates could be transformed to the corresponding alkene product with good to excellent reactivity and selectivity. The graphene encapsulated Ni@N/C catalyst also had good stability and can be applied in the industrially applicable flow reactor, which showed a promising method for ethylene synthesis in industry.

## ADDITIONAL INFORMATION

Corresponding Author

Email: [liujg@ms.giec.ac.cn](mailto:liujg@ms.giec.ac.cn); [mall@ms.giec.ac.cn](mailto:mall@ms.giec.ac.cn)

## Author Contributions

J.-G. L. and L.-L.M. conceived and designed the experiments. J.-G. L., J. M. S. and S.S. L. performed experiments, data analysis and prepared the Supplementary Information. J.-G. L. wrote the paper. All authors discussed the results and commented on the manuscript.

## ACKNOWLEDGMENT

This work was supported financially by the National Natural Science Foundation of China (Project 51976225), Dalian National Laboratory Cooperation Foundation, Chinese Academy of Sciences (Project DNL201916).

## REFERENCES

- [1] Prof. Dr. Johannes G. de Vries, P. D. C. J. E. *The Handbook of Homogeneous Hydrogenation*. (WILEY-VCH Verlag GmbH & Co. KGaA, 2006).
- [2] Crespo-Quesada, M., Cardenas-Lizana, F., Dessimoz, A. L. & Kiwi-Minsker, L. Modern Trends in Catalyst and Process Design for Alkyne Hydrogenations. *ACS Catal.* **2**, 1773-1786 (2012).
- [3] Michaelides, I. N. & Dixon, D. J. Catalytic Stereoselective Semihydrogenation of Alkynes to E-Alkenes. *Angew. Chem. Int. Ed.* **52**, 806-808 (2013).
- [4] Oger, C., Balas, L., Durand, T. & Galano, J. M. Are Alkyne Reductions Chemo-, Regio-, and Stereoselective Enough To Provide Pure (Z)-Olefins in Polyfunctionalized Bioactive Molecules? *Chem. Rev.* **113**, 1313-1350 (2013).

- [5] Delgado, J. A., Benkirane, O., Claver, C., Curulla-Ferre, D. & Godard, C. Advances in the preparation of highly selective nanocatalysts for the semi-hydrogenation of alkynes using colloidal approaches. *Dalton Trans.* **46**, 12381-12403 (2017).
- [6] Karunananda, M. K. & Mankad, N. P. E-Selective Semi-Hydrogenation of Alkynes by Heterobimetallic Catalysis. *J. Am. Chem. Soc.* **137**, 14598-14601 (2015).
- [7] Takale, B. S. *et al.* Unsupported Nanoporous Gold Catalyst for Chemoselective Hydrogenation Reactions under Low Pressure: Effect of Residual Silver on the Reaction. *J. Am. Chem. Soc.* **138**, 10356-10364 (2016).
- [8] Vile, G., Albani, D., Almora-Barrios, N., Lopez, N. & Perez-Ramirez, J. Advances in the Design of Nanostructured Catalysts for Selective Hydrogenation. *Chemcatchem* **8**, 21-33 (2016).
- [9] McCue, A. J., Guerrero-Ruiz, A., Ramirez-Barria, C., Rodriguez-Ramos, I. & Anderson, J. A. Selective hydrogenation of mixed alkyne/alkene streams at elevated pressure over a palladium sulfide catalyst. *J. Catal.* **355**, 40-52 (2017).
- [10] Benavidez, A. D. *et al.* Improved selectivity of carbon-supported palladium catalysts for the hydrogenation of acetylene in excess ethylene. *Appl. Catal., A* **482**, 108-115 (2014).
- [11] Chesnokov, V. V., Podyacheva, O. Y. & Richards, R. M. Influence of carbon nanomaterials on the properties of Pd/C catalysts in selective hydrogenation of acetylene. *Mater. Res. Bull.* **88**, 78-84 (2017).
- [12] Choe, K. *et al.* Fast and Selective Semihydrogenation of Alkynes by Palladium Nanoparticles Sandwiched in Metal-Organic Frameworks. *Angew. Chem. Int. Ed.* **59**, 3650-3657 (2020).
- [13] Chernichenko, K. *et al.* A frustrated-Lewis-pair approach to catalytic reduction of alkynes to cis-alkenes. *Nat. Chem.* **5**, 718-723 (2013).
- [14] Desai, S. P. *et al.* Well-Defined Rhodium-Gallium Catalytic Sites in a Metal-Organic Framework: Promoter-Controlled Selectivity in Alkyne Semihydrogenation to E-Alkenes. *J. Am. Chem. Soc.* **140**, 15309-15318 (2018).
- [15] Gorgas, N. *et al.* Efficient Z-Selective Semihydrogenation of Internal Alkynes Catalyzed by Cationic Iron (II) Hydride Complexes. *J. Am. Chem. Soc.* **141**, 17452-17458 (2019).
- [16] Ramirez, B. L. & Lu, C. R. Rare-Earth Supported Nickel Catalysts for Alkyne Semihydrogenation: Chemo- and Regioselectivity Impacted by the Lewis Acidity and Size of the Support. *J. Am. Chem. Soc.* **142**, 5396-5407 (2020).
- [17] Fu, S. M. *et al.* Ligand-Controlled Cobalt-Catalyzed Transfer Hydrogenation of Alkynes: Stereodivergent Synthesis of Z- and E-Alkenes. *J. Am. Chem. Soc.* **138**, 8588-8594 (2016).
- [18] Tokmic, K. & Fout, A. R. Alkyne Semihydrogenation with a Well-Defined Nonclassical Co-H<sub>2</sub> Catalyst: A H<sub>2</sub> Spin on Isomerization and E-Selectivity. *J. Am. Chem. Soc.* **138**, 13700-13705 (2016).
- [19] Gramigna, K. M., Dickie, D. A., Foxman, B. M. & Thomas, C. M. Cooperative H<sub>2</sub> Activation across a Metal-Metal Multiple Bond and Hydrogenation Reactions Catalyzed by a Zr/Co Heterobimetallic Complex. *ACS Catal.* **9**, 3153-3164 (2019).
- [20] Wang, Y. L., Huang, Z. D. & Huang, Z. Catalyst as colour indicator for endpoint detection to enable selective alkyne trans-hydrogenation with ethanol. *Nat Catal* **2**, 529-536 (2019).
- [21] Mitsudome, T. *et al.* One-step Synthesis of Core-Gold/Shell-Ceria Nanomaterial and Its Catalysis for Highly Selective Semihydrogenation of Alkynes. *J. Am. Chem. Soc.* **137**, 13452-13455 (2015).
- [22] Lu, Y. *et al.* Highly Selective Semihydrogenation of Alkynes to Alkenes by Using an Unsupported Nanoporous Palladium Catalyst: No Leaching of Palladium into the Reaction Mixture. *ACS Catal.* **7**, 8296-8303 (2017).
- [23] Meng, X. C. *et al.* Selective hydrogenation of nitrobenzene to aniline in dense phase carbon dioxide over Ni/gamma-Al<sub>2</sub>O<sub>3</sub>: Significance of molecular interactions. *J. Catal.* **264**, 1-10 (2009).
- [24] Polshettiwar, V., Baruwati, B. & Varma, R. S. Nanoparticle-supported and magnetically recoverable nickel catalyst: a robust and economic hydrogenation and transfer hydrogenation protocol. *Green Chem.* **11**, 127-131 (2009).
- [25] Tanabe, K. K. *et al.* Discovery of Highly Selective Alkyne Semihydrogenation Catalysts Based on First-Row Transition-Metallated Porous Organic Polymers. *Angew. Chem. Int. Ed.* **53**, 12055-12058 (2014).
- [26] Fedorov, A., Liu, H.-J., Lo, H.-K. & Coperet, C. Silica-Supported Cu Nanoparticle Catalysts for Alkyne Semihydrogenation: Effect of Ligands on Rates and Selectivity. *J. Am. Chem. Soc.* **138**, 16502-16507 (2016).
- [27] Liu, Y. *et al.* Layered double hydroxide-derived Ni-Cu nanoalloy catalysts for semi hydrogenation of alkynes: Improvement of selectivity and anti-coking ability via alloying of Ni and Cu. *J. Catal.* **359**, 251-260 (2018).
- [28] Jaiswal, G. *et al.* N-Graphitic Modified Cobalt Nanoparticles Supported on Graphene for Tandem Dehydrogenation of Ammonia-Borane and Semihydrogenation of Alkynes. *ACS Sustainable Chem. Eng.* **8**, 11058-11068 (2020).
- [29] Shi, X. *et al.* Fabrication of Ni<sub>3</sub>N nanorods anchored on N-doped carbon for selective semi-hydrogenation of alkynes. *J. Catal.* **382**, 22-30, (2020).
- [30] Lee, I., Joo, J. B., Yin, Y. D. & Zaera, F. A Yolk@Shell Nanoarchitecture for Au/TiO<sub>2</sub> Catalysts. *Angew. Chem. Int. Ed.* **50**, 10208-10211 (2011).
- [31] Holgado, J. P., Ternero, F., Gonzalez-delaCruz, V. M. & Caballero, A. Promotional Effect of the Base Metal on Bimetallic Au-Ni/CeO<sub>2</sub> Catalysts Prepared from Core-Shell Nanoparticles. *ACS Catal.* **3**, 2169-2180 (2013).
- [32] Li, Z. W., Mo, L. Y., Kathiraser, Y. & Kawi, S. Yolk-Satellite-Shell Structured Ni-Yolk@Ni@SiO<sub>2</sub> Nanocomposite: Superb Catalyst toward Methane CO<sub>2</sub> Reforming Reaction. *ACS Catal.* **4**, 1526-1536 (2014).
- [33] Movahed, S. K., Lehi, N. F. & Dabiri, M. Palladium nanoparticles supported on core-shell and yolk-shell Fe<sub>3</sub>O<sub>4</sub>@nitrogen doped carbon cubes as a highly efficient, magnetically separable catalyst for the reduction of nitroarenes and the oxidation of alcohols. *J. Catal.* **364**, 69-79 (2018).
- [34] Almeida, C. V. S., Tremiliosi, G., Eguiluz, K. I. B. & Salazar-Banda, G. R. Improved ethanol electro-oxidation at Ni@Pd/C and Ni@PdRh/C core-shell catalysts. *J. Catal.* **391**, 175-189 (2020).
- [35] Gao, J. *et al.* Ambient Hydrogenation and Deuteration of Alkenes Using a Nanostructured Ni-Core-Shell Catalyst. *Angew. Chem. Int. Ed.* (2021).
- [36] Kim, S., Lauterbach, J. & Sasmaz, E. Yolk-Shell Pt-NiCe@SiO<sub>2</sub> Single-Atom-Alloy Catalysts for Low-Temperature Dry Reforming of Methane. *ACS Catal.* **11**, 8247-8260 (2021).
- [37] Geim, A. K. & Novoselov, K. S. The rise of graphene. *Nat. Mater.* **6**, 183-191 (2007).
- [38] Castro Neto, A. H., Guinea, F., Peres, N. M. R., Novoselov, K. S. & Geim, A. K. The electronic properties of graphene. *Rev. Mod. Phys.* **81**, 109-162 (2009).
- [39] Wong, D. L. *et al.* Cascade of electronic transitions in magic-angle twisted bilayer graphene. *Nature* **582**, 198-202 (2020).
- [40] Park, J. M., Cao, Y., Watanabe, K., Taniguchi, T. & Jarillo-Herrero, P. Tunable strongly coupled superconductivity in magic-angle twisted trilayer graphene. *Nature* **590**, 249-255 (2021).
- [41] Liu, J. G. *et al.* Facile synthesis of controllable graphene-co-shelled reusable Ni/NiO nanoparticles and their application in the synthesis of amines under mild conditions. *Green Chem.* **22**, 7387-7397 (2020).
- [42] Guimon, C., Auroux, A., Romero, E. & Monzon, A. Acetylene hydrogenation over Ni-Si-Al mixed oxides prepared by sol-gel technique. *Appl. Catal., A* **251**, 199-214 (2003).
- [43] Wang, L., Li, F. X., Chen, Y. J. & Chen, J. X. Selective hydrogenation of acetylene on SiO<sub>2</sub>-supported Ni-Ga alloy and intermetallic compound. *J. Energy Chem.* **29**, 40-49 (2019).
- [44] Xu, Z., Zhou, S. & Zhu, M. Ni catalyst supported on nitrogen-doped activated carbon for selective hydrogenation of acetylene with high concentration. *Catal. Commun.* **149** (2021).
- [45] Liang, H. W., Wei, W., Wu, Z. S., Feng, X. L. & Mullen, K. Mesoporous Metal-Nitrogen-Doped Carbon Electrocatalysts for Highly Efficient Oxygen Reduction Reaction. *J. Am. Chem. Soc.* **135**, 16002-16005 (2013).
- [46] Xiong, W. *et al.* Nitrogen-doped carbon nanotubes as a highly active metal-free catalyst for nitrobenzene hydrogenation. *Appl. Catal., B* **260** (2020).
- [47] Chen, Y. & Chen, J. Selective hydrogenation of acetylene on SiO<sub>2</sub> supported Ni-In bimetallic catalysts: Promotional effect of In. *Appl. Surf. Sci.* **387**, 16-27 (2016).
- [48] Liu, J. Y., Chang, H. Y., Truong, Q. D. & Ling, Y. C. Synthesis of nitrogen-doped graphene by pyrolysis of ionic-liquid-functionalized graphene. *J. Mater. Chem. C* **1**, 1713-1716 (2013).
- [49] Greczynski, G. & Hultman, L. Compromising Science by Ignorant Instrument Calibration-Need to Revisit Half a Century of Published XPS Data. *Angew. Chem. Int. Ed.* **59**, 5002-5006 (2020).
- [50] Konnerth, H. & Precht, M. H. G. Selective partial hydrogenation of alkynes to (Z)-alkenes with ionic liquid-doped nickel nanocatalysts at near ambient conditions. *Chem. Commun.* **52**, 9129-9132 (2016).
- [51] Murugesan, K., Alshammari, A. S., Sohail, M., Beller, M. & Jagadeesh, R. V. Monodisperse nickel-nanoparticles for stereo- and chemoselective hydrogenation of alkynes to alkenes. *J. Catal.* **370**, 372-377 (2019).
- [52] Yang, L. *et al.* Semihydrogenation of phenylacetylene over nonprecious Ni-based catalysts supported on AISBA-15. *J. Catal.* **370**, 310-320 (2019).